Raman investigation of H$_2$O molecule and hydroxyl groups in the channels of hemimorphite

BORIS KOLESOV*

Institute of Inorganic Chemistry, Russian Academy of Sciences, Lavrentiev av. 3, Novosibirsk 630090, Russia

ABSTRACT

Single-crystal polarized Raman spectra (40 to 4000 cm^{-1} at $4 \leq T \leq 860$ K) were measured for hemimorphite, Zn$_4$Si$_2$O$_7$(OH)$_2$·H$_2$O, to determine the behavior of H$_2$O molecules and OH groups in the channels. All observed stretching modes of the O-H vibrations could be assigned. Low-temperature Raman spectra show the presence of two different spatially divided regions in the crystal where the H$_2$O molecules and hydroxyl groups have slightly different positions in the channel. Two structural phase transitions were observed at 20–30 and 80–100 K, respectively, which reflect temperature replacement and reorientation of the H$_2$O molecules in the cavity. At $T > 100$ K, H$_2$O molecules are rotationally disordered around the **c** axis. An analysis of combined modes consisting of external and internal H$_2$O vibrations permits the frequency of translational T(H$_2$O) modes at 30, 53, 71, 90, 118, and 148 cm^{-1} to be determined. The T(H$_2$O) modes also can be observed directly at low frequencies in the Raman spectra. The dehydration process of hemimorphite was investigated by Raman measurements at elevated temperatures of the crystal. One of two hydroxyl groups in the dehydrated crystal is hydrogen-bonded to neighbor oxygen and disordered statistically.

Keywords: Hemimorphite, H$_2$O molecules, microporous minerals, Raman spectroscopy

INTRODUCTION

There is considerable interest at the present time in understanding the nature of molecular fluids in various environmental and low-temperature geological systems. Surface reactions on minerals and rocks, and mineral weathering and dissolution are examples of the types of low-temperature geological processes that are controlled principally by the behavior of H$_2$O-rich fluids and their interaction with solid Earth materials.

However, the nature of local molecule-mineral interactions is so complex that an interpretation of many experimental data, and even more importantly obtaining quantitative physical understanding, is often difficult if not impossible. Thus, it is necessary to investigate "simple systems" to establish some physical scientific basis before more complicated systems can be investigated. It is here that studies of the H$_2$O molecule in micro and nanoporous minerals and inner-surface-type interactions can be extremely useful. This is because either a single or a small number of H$_2$O molecules are contained in the micro and nanopores of a crystalline structure, often in a structurally ordered way. As a result, it is easier to understand the nature of their molecule-mineral interactions compared to those occurring on outer surfaces and that are highly disordered.

Hemimorphite, Zn$_4$Si$_2$O$_7$(OH)$_2$·H$_2$O, is a low-temperature phase typically found in oxidized zones of zinc ore deposits. The hemimorphite crystal structure is characterized by relatively small cavities that contain single H$_2$O molecules (McDonald and Cruickshank 1967 and reference therein). The molecules lie in the

(010) plane with their rotation axes parallel to [001]. Within the cavities, the H$_2$O molecules are hydrogen bonded to two O atoms as a donor of hydrogen bonds, i.e., acid, and two H atoms as an acceptor of hydrogen bonds, i.e., base, both of which are part of the framework (Fig. 1b). Thus, all the donor and acceptor sites of the H$_2$O molecule are bonded (Hill et al. 1977; Takeuchi et al. 1978). From this point of view, the arrangement of the water molecule in hemimorphite at room temperature could be described as "two-dimensional ice" because all four hydrogen bonds of the H$_2$O in the cavity are coplanar. The hydrogen bonds between the H$_2$O molecule and the framework O atoms (O3 atoms) are weaker than those between the H$_2$O molecule and the OH groups (H3 atoms). It confirms the well-known rule that the water is a strong acceptor and a relatively weak donor of hydrogen bonds (Jeffrey 1997, p. 59). At low temperature, the water molecule is displaced from the center of the cavity to the side of the **a-c** plane (Libowitzky et al. 1998). Only two relatively strong bonds remain in the water molecule: one donor hydrogen bond with O3 atom and one acceptor hydrogen bond with hydroxyl group (Fig. 1a). Upon heating hemimorphite at 1 atm, H$_2$O loss occurs in two stages (Faust 1951; Taylor 1962): molecular H$_2$O starts to be expelled around 570 K and is completely gone around 770 K. During dehydration, the structural framework undergoes only minor adjustments. In the second stage, dehydration occurs at about 930 K and, ultimately, a reconstructive transformation to the anhydrous phase β-Zn$_2$SiO$_4$ occurs (Taylor 1962).

At room temperature, hemimorphite is orthorhombic, space group *Imm*2 with $Z = 2$ (McDonald and Cruickshank 1967). The zone center vibrations at the Γ point are described by irreducible representation:

$$\Gamma = 14\,A_1 + 10\,A_2 + 12\,B_1 + 12\,B_2$$
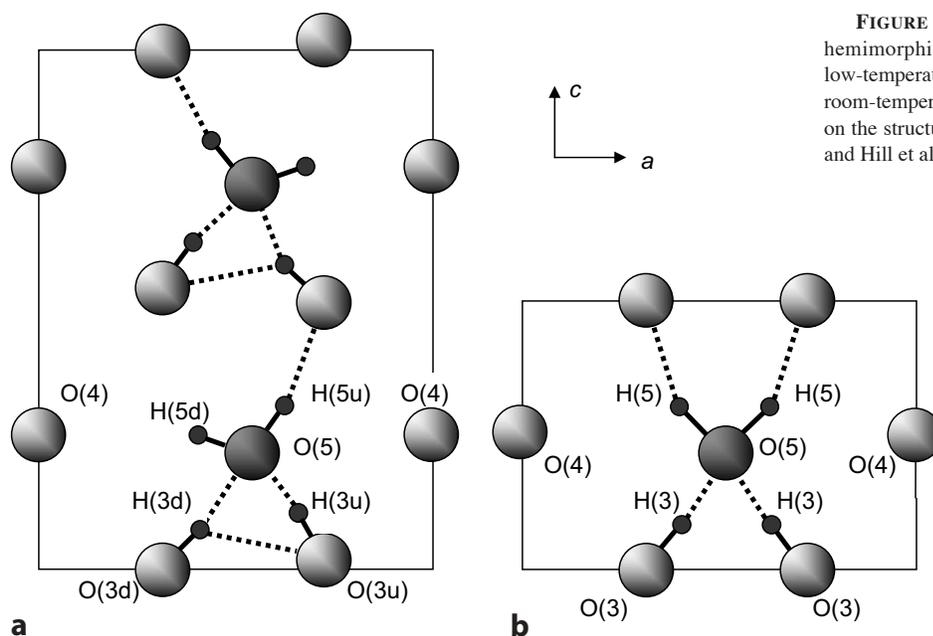
* E-mail: kolesov@che.nsk.su

All modes are Raman and IR active except the A$_2$ modes, which are inactive in the infrared.

At low temperature, the H$_2$O molecules in hemimorphite occupy general crystallographic positions (Fig. 1a). The H$_2$O has different strengths of hydrogen bonding with its local surroundings in the cavity, and its symmetry is C_{1h} compared to C_{2v} for a free H$_2$O molecule and H$_2$O in the cavity at room temperature. All H$_2$O vibrational modes, three internal and six external, are active in the IR and Raman for both low- and room-temperature arrangements.

In comparison to the number of X-ray and neutron diffraction studies made on hemimorphite to date (Libowitzky et al. 1998 and references therein), there have been few vibrational spectroscopic investigations. The vibrational (IR) properties of the H$_2$O measured on very thin oriented slices of hemimorphite were investigated by Libowitzky and Rossman (1996, 1997) over the temperature range of 82–373 K. They analyzed the symmetry and energy of the O-H stretching and bending modes of the O-H in the framework and of the H$_2$O in the channels of hemimorphite. They proposed the existence of a phase transition at around 100 K based on a discontinuity in optical birefringence values and vibrational mode behavior. It is necessary to note, however, that the stretching modes in hemimorphite are still significantly broadened at 80 K and some of them are overlapped and, therefore, the IR spectra have some inherent uncertainty. Libowitzky et al. (1998) proposed also that the crystal lattice at 20 K could be described by an order-disorder structural model with microdomains and twinning. Therefore, the present work was undertaken to study the behavior of the H$_2$O molecule in the hemimorphite channels at low temperature and to investigate the nature of the phase transition occurring around 100 K. To do this in a detailed way, single-crystal polarized Raman spectra were measured over both a wide spectral ($\Delta\omega = 40$–4000 cm^{-1}) and wide temperature (4–860 K) range.

EXPERIMENTAL METHODS

The crystals of hemimorphite used for study were obtained from the mineral collection of Kiel University, Germany. The crystals had a specific wedge-shaped form and could be oriented easily. For the Raman measurements, single crystals were removed and cut such that small oriented platelets of about 3 × 2 × 0.5 mm were obtained.

The Raman spectra were collected using a triple grating spectrometer with a CCD detector, LN-1340PB, from Princeton Instruments, U.S.A., Spectral calibration of the spectrometer was performed each time with the lines of a Ne-lamp. The 488 nm line of an Ar$^+$ laser was used for the spectral excitation, with the diameter of the laser spot on the sample surface being 1–2 μm. The laser power at the sample was typically 5–10 mW. The spectra at all temperatures were measured in 180° back-scattering collection geometry with a Raman microscope. The low-temperature spectra were recorded by mounting the crystal on a cold finger of a helium cryostat (MicrostatHe) from Oxford Instruments. The precision of the measured temperatures of the cold finger is of 0.1 K, but the true temperature of the sample can differ from the measured one due to some heating of the sample in the laser spot. We estimate this heating as 1–2 K for transparent crystals. All measurements were performed with a spectral resolution of 2 cm^{-1} at low temperature (4 K) and 5 cm^{-1} at other temperatures.

RESULTS

Figures 2a, 2b, and 2c show single-crystal polarized Raman spectra of hemimorphite at room temperature in the different spectral regions. The spectra of O-H stretching vibrations (Fig. 2c) consist of few overlapped and broadened bands, and it is rather difficult to extract some helpful information from them.

Figures 3a and 3b show the polarized spectra of the O-H stretching vibrations at 4 K taken in different areas of the sample surface (the small diameter of the laser beam, i.e., 1–2 μm, permits analysis of the crystal in individual micrometer-sized areas). The spectrum at Figure 3a is characterized by a set of the bands at $\Delta\omega$ = ~3370, 3398, 3581, and 3616 cm^{-1} (Set I). The spectrum at Figure 3b is characterized, however, by two sets of the bands. Set I is the same as in Figure 3a, whereas Set II involves the bands at $\Delta\omega$ = 3342, 3390, 3554, 3571, and 3600 cm^{-1} (Set II). The bands from Set I and Set II are labeled in Figures 3a
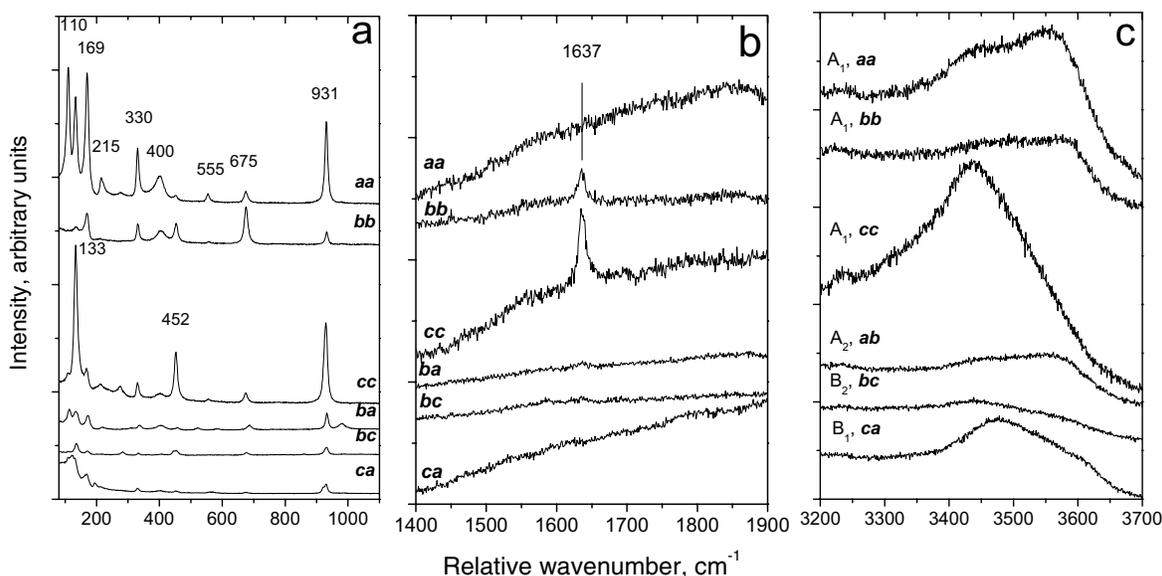
FIGURE 2. Polarized single-crystal Raman spectra of the lattice (**a**), H$_2$O bending (**b**), and O-H and H$_2$O stretching (**c**) modes in hemimorphite at 295 K.
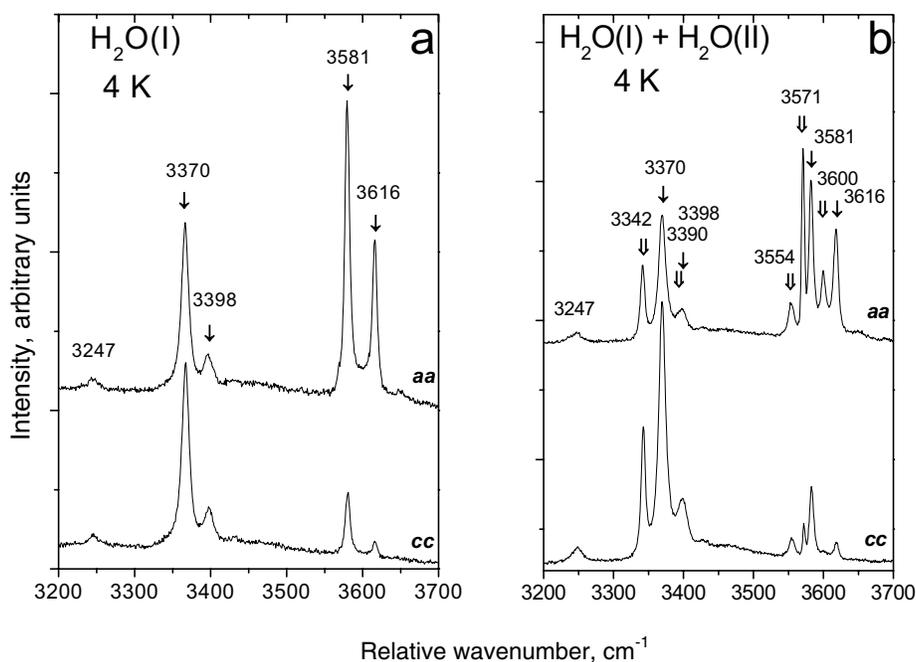

FIGURE 3. Polarized single-crystal Raman spectra of the O-H and H$_2$O stretching modes in hemimorphite at 4 K taken in different areas of the crystal surface. The features labeled by single arrows comprise the bands of Set I, which characterize the H$_2$O(I) state of the H$_2$O molecule and hydroxyl groups in the cavity; double arrows label the bands of Set II, which characterize the H$_2$O(II) state. One can see that the spectra represented in **a** involve only the bands of Set I, whereas the spectra in **b** involve the bands of both Sets I and II.

and 3b by single and double arrows, respectively. Obviously, these sets describe two different arrangements of the water molecule and O-H groups in the cavity, H$_2$O(I) and H$_2$O(II), respectively. Thus, Figure 3a represents the stretching vibrations of the H$_2$O(I), whereas Figure 3b involves the vibrations of both states of the H$_2$O molecule, H$_2$O(I) and H$_2$O(II). The difference between these two states is not significant and can be described

by the shift of some bands to lower energy [e.g., the band at $\Delta\omega$ = ~3370 cm^{-1} from Set I shifts to the band at $\Delta\omega$ = 3342 cm^{-1} from Set II, the band at $\Delta\omega$ = 3398 cm^{-1} (Set I) shifts to $\Delta\omega$ = 3390 cm^{-1} (Set II), etc.]. All low-frequency bands of both sets (i.e., in the range of $\Delta\omega$ = 3300–3500 cm^{-1}) relate to the vibration of the bonds elongated preferentially along the **c**-axis, whereas the high-frequency bands ($\Delta\omega$ = 3500–3700 cm^{-1}) relate to the

vibration of the bonds elongated along the *a*-axis.

The weak band at $\Delta\omega = 3247$ cm^{-1} is assigned to the overtone of H$_2$O bending mode ν_2 ($\Delta\omega = 1642$ cm^{-1} at 4 K), enhanced in intensity through Fermi resonance.[1] In addition, a few weak and broad bands are observed in the frequency range of $\Delta\omega = 3400$–3550 cm^{-1} (Fig. 4). These bands do not demonstrate any preferential orientation in the cavity, but they are "attached" to the band at $\Delta\omega = 3398$ cm^{-1} (Set I): shift of the latter down by 6–8 cm^{-1} (i.e., to $\Delta\omega = 3390$ cm^{-1}) leads to the same shift of the all weak bands. The weak bands are attributed to a combined mode of H$_2$O internal (i.e., stretching mode at $\Delta\omega = 3398$ cm^{-1}) and external vibrations.

Figures 5a and 5b show temperature dependent *aa*- and *cc*-spectra of the O-H stretching modes in the range of 4–295 K. Two-phase transitions are seen clearly. The first one occurs between 10 and 30 K and is manifested by the disappearance of the bands at $\Delta\omega = 3342$, 3554, and 3571 cm^{-1} from the Set II. The second phase transition is observed at 80–100 K. The lowest frequency mode (i.e., at $\Delta\omega = 3370$ cm^{-1}) and the highest frequency mode (i.e., at $\Delta\omega = 3616$ cm^{-1}) become weaker in intensity at $T > 90$ K, and an additional mode at $\Delta\omega = \sim3500$ cm^{-1} arises (labeled by the arrow in Figs. 5a and 5b). In addition, all low-frequency modes show some increasing trend in peak position under heating, whereas the high-frequency modes show some decreasing trend in peak position. Thus, an increase of temperature from 4 to 295 K leads to a weakening of the strong hydrogen-bonded bonds and a strengthening of the weak-bonded bonds of the H$_2$O molecules and the hydroxyl groups.

Figure 6 shows the temperature-dependent spectra in the range of H$_2$O bending vibration. There are two modes at low temperature with $\Delta\omega = 1642$ and 1837 cm^{-1}. The mode at 1642 cm^{-1} is typically assigned to the bending vibration of hydrogen-

bonded H$_2$O molecules. The mode at 1837 cm^{-1} spreads into the broad band of weak intensity at $T > 100$ K.

The lower-frequency spectra of the lattice vibrations vs. temperature are shown in Figure 7a. Many of the bands observed at 4 K spread significantly between 80 and 100 K (i.e., in the range of the second phase transition) giving rise to a steady continuum at $\Delta\omega = 40$–150 cm^{-1} at room temperature (solid spectrum in Fig. 7b, where the continuum is shown by the hatched area).

Figure 8a shows the unpolarized spectra at elevated temperature. After complete dehydration of the crystal occurring at 860 K, the spectrum exhibits just two bands at $\Delta\omega = 3529$ and 3604 cm^{-1} (Fig. 8b). At low temperature, the mode at $\Delta\omega = 3529$ cm^{-1} decreases in frequency up to 3506 cm^{-1}, but the mode at $\Delta\omega = 3604$ cm^{-1} is kept nearly constant (Fig. 8b). The low-frequency band, i.e., $\Delta\omega = 3529$ cm^{-1}, is broadened significantly and asymmetrical in shape at room temperature.

DISCUSSION

H₂O stretching vibrations

The spectrum of the H$_2$O(I) represented in Figure 3a is consistent completely with results of neutron diffraction (Fig. 1a). Two low-frequency bands at $\Delta\omega = \sim3370$ and 3398 cm^{-1} are caused by O3-H3u···O5 and O5-H5u···O3 stretchings respectively, whereas the high-frequency modes at $\Delta\omega = 3581$ and 3616 cm^{-1} are caused by O3-H3d (weak hydrogen bond) and O5-H5d (non-hydrogen-bonded) stretchings, respectively. This assignment is in accord with bond lengths (Libowitzky et al. 1998), bond directions (Fig. 1a), and the fact that the observed combined internal-external water vibrations (Fig. 4 and section "External vibrations") are "attached" to the band at $\Delta\omega = 3398$ cm^{-1}, i.e., the H$_2$O stretching.

The spectrum of the H$_2$O(II), characterized by the modes at $\Delta\omega = 3342$, 3390, 3554, 3571, and 3600 cm^{-1} (Fig. 3b), is assigned satisfactorily by the same H$_2$O arrangement in the cavity. Table 1 lists the assignment of the observed O-H stretching vibrations of the H$_2$O(I) and H$_2$O(II) molecules and hydroxyl groups in low-temperature hemimorphite. There are, however, two questions: (1) what is the difference between the two observed states of the water molecule, and (2) why are there three bands in the high-frequency range (i.e., $\Delta\omega = 3554$, 3571, and 3600 cm^{-1}) of the spectrum of the H$_2$O(II) instead of two bands (i.e., $\Delta\omega = 3581$ and 3616 cm^{-1}) in the spectrum of the H$_2$O(I) (Figs. 3a and 3b, Table 1)?

From two low-frequency bands, i.e., $\Delta\omega = \sim3370$ and 3398 cm^{-1}, both relating to the H$_2$O(I), the first band differs from the analogous band of the H$_2$O(II), i.e., $\Delta\omega = 3342$ cm^{-1}, by ~30 cm^{-1}, whereas the second one differs from its counterpart in the spectrum of the H$_2$O(II), i.e., band at $\Delta\omega = 3390$ cm^{-1}, by only 8

---

[1] The frequency of the overtone is less than twice the frequency of the main tone due to an anharmonicity of vibrations and interaction of the overtone with the H$_2$O stretching mode of the same symmetry (i.e., ν_1), which shifts the former to lower energy (e.g., Aoki et al. 1995).
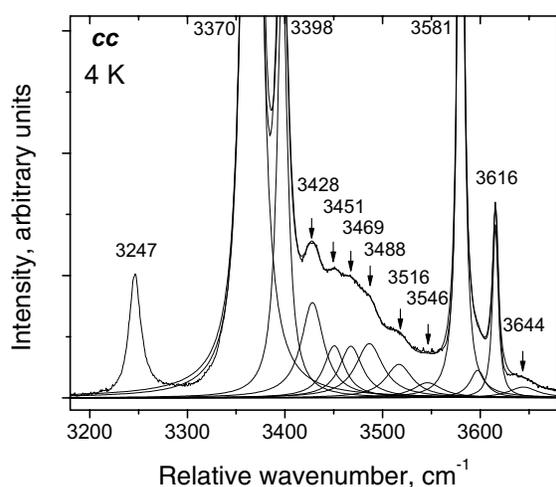

FIGURE 4. Result of curve fitting of the low-temperature *cc*-spectrum of the H$_2$O(I) stretching vibrations in hemimorphite.

TABLE 1. Peak position (in cm^{-1}) of the observed O-H stretching modes for the H$_2$O(I) and H$_2$O(II) states of the water molecules in hemimorphite at 4 K and their assignment

H₂O(I)	H₂O(II)	Assignment
~3370	3342	O(3u)-H(3u)···O(5)
3398	3390	O(5)-H(5u)···O(3)
3581	3554	O(3d)-H(3d)···O(5)
–	3571	O(3d)-H(3d)···O(3u)
3616	3600	O5-H(5d)

cm^{-1} (Table 1). This difference means that the H₂O(II) is characterized by a shorter distance between O3H3u and O5 compared to that of the H₂O(I), whereas the O5H5u···O3 distance remains nearly unchanged. High-frequency modes at $\Delta\omega = 3581$ and 3616 cm^{-1} of H₂O(I) are shifted to 3554 and 3600 cm^{-1} of H₂O(II), respectively (Table 1), which means that the O3d···O5 distance for H₂O(II) is shortened. The bond direction for both H₂O states can be estimated from the intensity of the corresponding bands in the polarized spectra. The ratio I(*aa*)/I(*cc*) of the integral intensity of the band at $\Delta\omega = 3554$ cm^{-1} [H₂O(II)] in the *aa*- and *cc*-spectra as well as the similar ratio of the band at $\Delta\omega = 3581$ cm^{-1} [H₂O(I), Fig. 3a and 3b] shows that the O3d-H3d bond associated with the H₂O(II) is inclined with respect to *c*-axis to a lesser extent than this bond associated with the H₂O(I). This difference can indicate some small displacement of O3d atom in *a*-direction toward O3u oxygen. The latter initiates the appearance of the additional O3d-H3d···O3u hydrogen bonding and additional band at 3571 cm^{-1} in the spectrum of the H₂O(II). Libowitzky et al. (1998) stated that H3d atom has large thermal parameter $U_{33} = 4.38 \cdot 10^{-2}$ Å^2 at 20 K and can be modeled by a split-atom site. Since the lifetime of the H3d atom in each position should be greater than the frequency of the stretching vibration, i.e., $\sim 10^{-14}$ s, and the time scale associated with Raman scattering is roughly 10^{-15} s, both split states of the H3d atom should be observed in the Raman spectra as individual bands. One can propose, therefore, that the modes at $\Delta\omega = 3554$ and 3571 cm^{-1} in the spectrum of the H₂O(II) are assigned to the stretching vibration of the H3d split-atom site with the greater character of the O3d-H3d···O5 in the former, and the O3d-H3d···O3u in the latter. One can propose also that the structural model represented by Libowitzky et al. (1998) relates to the unit cell containing H₂O(II), which differs from the unit cell with H₂O(I) by the slightly shortened distances between atoms in the O3d···O3u···O5 triangle.
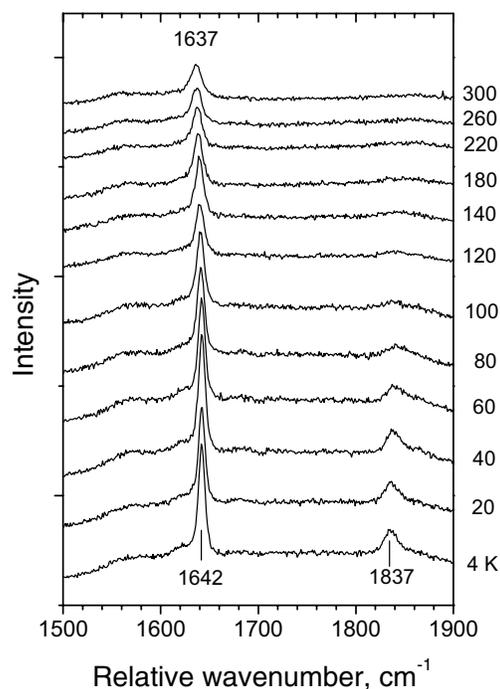

FIGURE 6. The spectra of H₂O bending vibration vs. temperature.

Temperature dependence

The temperature dependence of the polarized Raman spectra (Fig. 5a and 5b) shows the presence of two phase transitions in hemimorphite in the range of 4–300 K. A low-temperature phase transition is observed at ~20 K and is characterized by the disappearance of the areas in the crystal containing the H₂O(II), i.e., the disappearance of the modes at $\Delta\omega = 3342$, 3554, 3571, and 3600 cm^{-1}. Thus, the disturbance of the crystal lattice manifested
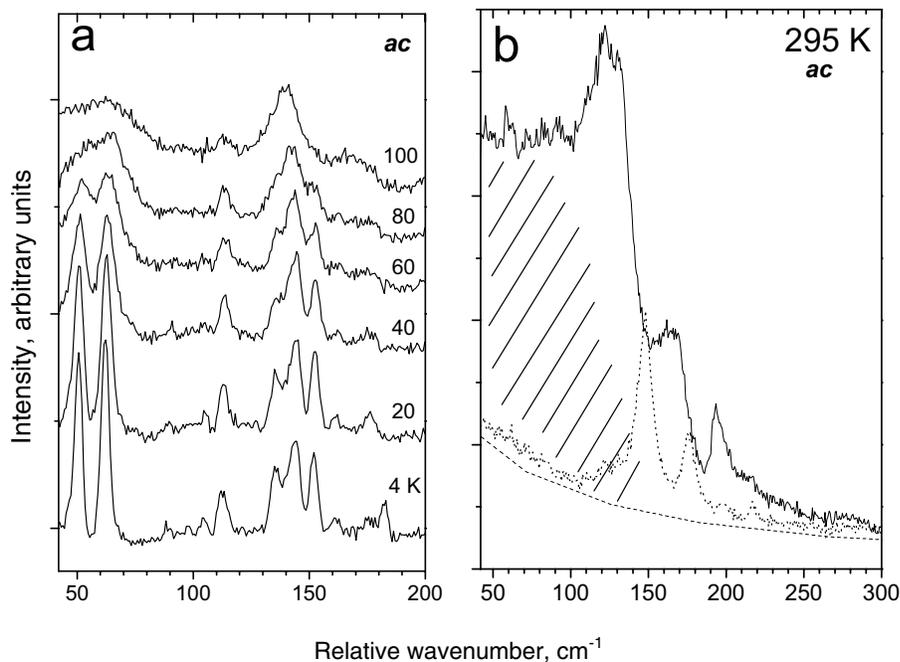
FIGURE 7. (**a**) A stacked plot of the polarized ***ac***-spectra ($4 \leq T \leq 100$ K) in the low-frequency region of the crystal lattice and H_2O translational vibrations in hemimorphite. (**b**) Room-temperature ***ac***-spectra of the natural (top spectrum in solid) and dehydrated (bottom spectrum in dotted) samples. The baseline for both spectra is shown by the dashed curve. The hatched area corresponds to the scattering on external (translational) vibrations of the H_2O molecule.
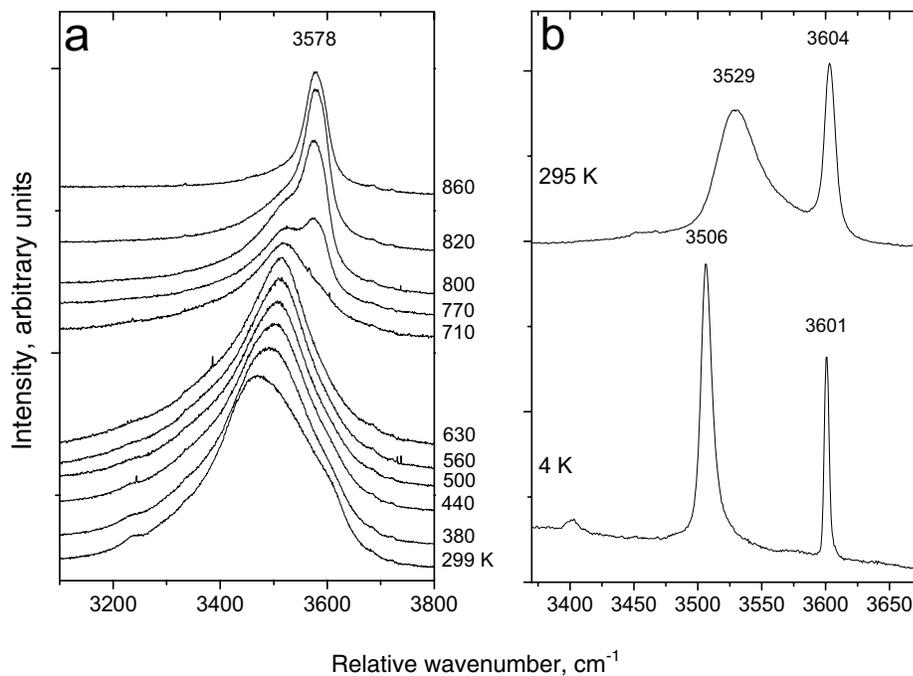

FIGURE 8. The unpolarized spectra of O-H and H_2O stretching modes in hemimorphite at elevated temperatures (**a**) and the spectra of O-H stretching vibrations of dehydrated hemimorphite (**b**).

by displacement of the O3uH3u hydroxyl group takes place just in part of the crystal and at very low temperature (less than 20 K). This observation is consistent with the assumption of Libowitzky et al. (1998) on the microdomain structure of the crystal at low temperature. However, the reason why some areas in the crystal behave differently from others is not clear. Possibly, this relates to some structural instability of the Zn atoms because these cations are bonded with the hydroxyl groups and preset the location of the latter in the lattice.

The other phase transition is observed at ~90 K and is ac-companied by the appearance of the broadened and overlapped bands, which are assigned to the mixed modes of ν_1 and ν_3 vibrations of a symmetrical water molecule at 3500–3600 cm^{-1}, and in-phase and out-of-phase vibrations of OH-groups at 3400–3500 cm^{-1}. Thus, the second structural phase transition is described by the displacement of the water molecule to center of the cavity (i.e., from the asymmetrical position depicted in Fig. 1a to the symmetrical one depicted in Fig. 1b). This phase transition was studied carefully by Libowitzky and Rossman (1997).

External vibrations

Figure 4 shows the deconvolution of the *cc*-spectrum of the H$_2$O(I) taken at 4 K with Lorentz components. Six distinct weak and broadened bands (compare to the main features) can be seen in the range between 3420 and 3560 cm^{-1}. As mentioned above (section "Results"), they are "attached" to the stretching of H$_2$O at $\Delta\omega = 3398$ cm^{-1} (i.e., these bands make up the high-frequency shoulder of the band at $\Delta\omega = 3398$ cm^{-1} and shift together with the latter) and should be attributed to combined modes of the H$_2$O internal (i.e., stretching) and external vibrations. The peak position of these bands (i.e., $\Delta\omega = 3428, 3451, 3469, 3488, 3516$, and 3546 cm^{-1}; Fig. 4) allows the frequency of the external modes to be extracted (30, 53, 71, 90, 118, and 148 cm^{-1} respectively). The order of magnitude of these frequencies indicates that all observed external modes are translational vibrations of H$_2$O molecules, T(H$_2$O). Since the unit cell of hemimorphite contains two water molecules at low temperature (Libowitzky et al. 1998; Fig. 1a), we observe a complete number of water translations in the lattice. Librational modes of H$_2$O, R(H$_2$O), should have a frequency greater than 200 cm^{-1}. [The librational frequency of the H$_2$O in beryl, where the molecule is almost free, is 190–210 cm^{-1} (Kolesov and Geiger 2000), and the frequency of hydrogen-bonded water molecules in liquid water is 300–900 cm^{-1} (Eisenberg and Kauzmann 1969).] The weak band at $\Delta\omega = \sim3644$ cm^{-1} (Fig. 4) is either R(H$_2$O) combined with the stretching vibration at $\Delta\omega = 3398$ cm^{-1} (in this case, the frequency of the librational mode is 246 cm^{-1}) or, more likely, T(H$_2$O) combined with the other stretching mode of H$_2$O, i.e., $\Delta\omega = 3615$ cm^{-1}, with a T(H$_2$O) frequency around 30 cm^{-1} (Table 2).

The external modes of H$_2$O can be observed directly in the low-frequency part of the spectra of the lattice vibrations. Figure 7a shows polarized (*ac*) temperature-dependent spectra in the range of $\Delta\omega = 40$–200 cm^{-1}. Many of the observed bands show a considerable broadening between 80 and 100 K (i.e., in the range of the second phase transition) and transform to a steady continuum at $\Delta\omega = 40$–150 cm^{-1} at room temperature (solid spectrum in Fig. 7b, where the continuum is shown by the hatched area). The appearance of a spectral continuum instead of distinct Raman bands is evidence for significant disordering of water molecules in the cavity at $T > 100$ K (see also next section). The observed continuum disappears completely after dehydration of the sample for 20 min at 860 K (dotted spectrum in Fig. 7b).

TABLE 2. H$_2$O translational modes defined from the analysis of the high-frequency combined bands (column 1) and the modes observed at lower wavenumbers in the Raman spectra (column 2), cm^{-1}

1	2
H$_2$O translations obtained from the analysis of the combined modes	The modes observed in the lowest frequency range of the lattice vibrations
30	
53	52
	62
71	
90	89
	98
	105
118	122
	135
148	152

Note: All listed frequencies are obtained at $T = 4$ K.

Thus, some of the low-frequency bands, which participate in the formation of the spectral continuum, can be assigned to pure translational motion of the water molecules in the cavity. The other ones should be assigned to mixed T(H$_2$O)-crystal lattice vibrations or pure lattice vibrations because the lowering of the crystal symmetry at low temperature (Libowitzky et al. 1998) gives rise to the appearance of the lattice modes forbidden for the high-temperature structure and it is difficult to solve, which bands are attributed to water molecule vibrations and to lattice vibrations, respectively.

Table 2 lists the frequencies of the H$_2$O translations determined from the combined H$_2$O internal-external bands (column 1) and the peak positions of all bands observed in the lower frequency spectra at 4 K (column 2). One can see that some frequencies obtained by these two different ways are nearly the same. The lowest frequency modes at ~ 30 cm^{-1} obtained from the analysis of the combined scattering (column 1) have no counterpart in the low-frequency Raman spectra (column 2) because of technical reasons, i.e., the restriction of the spectrograph spectral range.

H$_2$O bending vibrations

The bending mode at $\Delta\omega = 1642$ cm^{-1} shows strong intensity in *cc*-, intermediate in *bb*-, and weak in *aa*-spectra for all temperatures from 4 (Figs. 2b and 6) to 295 K. The mode at $\Delta\omega = 1642$ cm^{-1} is accompanied at low temperature by the mode at $\Delta\omega = 1837$ cm^{-1}. The latter spreads into the broad band of weak intensity at $T > 100$ K, i.e., after the second phase transition (Fig. 6). This behavior permits us to assign the band at $\Delta\omega = 1837$ cm^{-1} to a combined mode of the bending vibration at 1642 cm^{-1} and an external water molecule vibration with a frequency of 195 cm^{-1}. The frequency of 195 cm^{-1} is greater than the one determined for the translational mode of H$_2$O (see section "External vibrations" and Table 2), but less than would be expected for the frequency of the rotational modes. One can propose, therefore, that the mode at 195 cm^{-1} is a mixture between translational and rotational modes. A mixed mode arises typically when a molecule has to be displaced in some direction during rotational motion and vice versa. In addition, the assignment of the observed mode at 195 cm^{-1} to a mixed rotational-translational motion makes it clear why the mode couples with the bending vibration (1642 cm^{-1}), and why it has a relatively high intensity in the spectra. (The Raman intensity of the mode arises mainly from the modulation of the hydrogen bond, i.e., O5···O3 distance, during the vibration.) The spreading of the combined mode at 1837 cm^{-1} at $T > 100$ K can signify the rotational disorder of the H$_2$O molecule within some angle around the *c*-axis. The structural data of Hill et al. (1977) include indirect evidence of this suggestion manifested as too large a dimension of the thermal ellipsoid of the H and O atoms of H$_2$O at room temperature presented in the article. The conclusion about the rotational disorder of H$_2$O at $T > 100$ K in the channels also matches well with the observation of the translational disordering of H$_2$O (previous section) because both types of disordering are directly linked.

Dehydrated hemimorphite

The spectra of the stretching vibrations of the hydroxyl groups in dehydrated hemimorphite are represented in Figure

8b. Polarized spectra (not shown here) indicate that the band at $\Delta\omega = 3604$ cm^{-1} corresponds to the vibration of the bond directed between the *a*- and *c*-axes, whereas the band at $\Delta\omega = 3529$ cm^{-1} corresponds to the band directed preferentially along the *a*-axis. It is consistent with IR spectra and X-ray structure refinement data of Libowitzky et al. (1997). The high-frequency mode at 3604 cm^{-1} is assigned to the stretching of the O-H bond directed between *a*- and *c*-axis and having no hydrogen bonding in the surroundings. This lack of hydrogen bonding is the reason that its frequency barely changes with temperature. The other band, $\Delta\omega = 3529$ cm^{-1}, is attributed to the O-H group, the proton of which is directed to the other O3 atom, and thus, produces a weak hydrogen bond with the latter. Due to shortening of the distance between O3 atoms with cooling, the hydrogen bonding becomes stronger, and thus the mode frequency is lower than the one at ambient temperature (the frequency of O-H stretching vibrations is inversely proportional to the strength of hydrogen bonding). Both bands, $\Delta\omega = 3529$ and 3604 cm^{-1}, exhibit an asymmetrical shape with an overextended high-frequency wing, which is particularly marked at ambient temperature for the band at $\Delta\omega = 3529$ cm^{-1} (Fig. 8b). Such a shape of the vibrational band, which is observed rather rarely in vibrational spectra, is evidence for the static disorder of the hydrogen-bonded proton relative to the acceptor O3 atom. Indeed, one can suggest that the frequency of the band maximum reflects the shortest H⋯O3 distance, where the O-H⋯O angle is ~180° and the O-H bond is directed along the *a*-axis. Any departure of the H-atom from this position will cause the hydrogen bond to weaken and the O-H frequency to increase. This causes the appearance of the high-frequency extended wing of the band, which is observed in Figure 8b. The width of the wing corresponds roughly to the distribution of the proton over the positions near the O3 from slightly hydrogen-bonded to fully non-bonded. As seen in Figure 8b, the disordering of the hydrogen-bonded proton is much less at 4 K than at room temperature. The spectra in Figure 8b do not contain any evidence for the other (non-hydrogen-bonded) proton disordering; the slight asymmetry in the shape of the band at $\Delta\omega = 3604$ cm^{-1} can be derived from the site distribution of the neighbor (hydrogen-bonded) proton, which influences the vibrational frequency of the non-hydrogen-bonded proton through a mechanism of coupling.

REFERENCES CITED

Aoki, K., Yamawaki, H., and Sakashita, M. (1995) Pressure-turned Fermi resonance in ice VII. Science, 268, 1322–1324.

Eisenberg, D. and Kauzmann, W. (1969) The structure and properties of water. Oxford University Press, New York.

Faust, G.T. (1951) Thermal analysis and X-ray studies of sauconite and of some zinc minerals of the same paragenetic association. American Mineralogist, 36, 795–822.

Hill, R.J., Gibbs, G.V., Craig, J.R., Ross, F.K., and Williams, J.M. (1977) A neutron-diffraction study of hemimorphite. Zeitschrtift für Kristallaographie, 146, 241–259.

Jeffrey, G.A. (1997) An introduction to hydrogen bonding, 303 p. Oxford University Press, New York.

Kolesov, B.A. and Geiger, C.A. (2000) The orientation and vibrational states of H$_2$O in synthetic alkali-free beryl. Physics and Chemistry of Minerals, 27, 557–564.

Libowitzky, E. and Rossman, G.R. (1996) FTIR spectroscopy of lawsonite between 82 and 325 K. American Mineralogist, 81, 1080–1091.

——— (1997) IR spectroscopy of hemimorphite between 82 and 373 K and optical evidence for a low-temperature phase transition. European Journal of Mineralogy, 9, 793–802.

Libowitzky, E., Kohler, Th., Armbruster, Th., and Rossman, G.R. (1997) Proton disorder in dehydrated hemimorphite—IR spectroscopy and X-ray structure refinement at low and ambient temperatures. European Journal of Mineralogy, 9, 803–810.

Libowitzky, E., Schultz, A.J., and Young, D.M. (1998) The low-temperature structure and phase transition of hemimorphite, Zn$_4$Si$_2$O$_7$(OH)$_2$·H$_2$O. Zeitschrift für Kristallographie, 213, 659–668.

McDonald, W.S. and Cruickshank, D.W.J. (1967) Refinement of the structure of hemimorphite. Zeitschrift für Kristallographie, 124, 180–191.

Takeuchi, Y., Sasaki, S., Joswig, W., and Fuess, H. (1978) X-ray and neutron diffraction study of hemimorphite. Proceedings of the Japan Academy, Series B, 54, 577–582.

Taylor, H.F.W. (1962) The dehydration of hemimorphite. American Mineralogist, 47, 932–944.